

Toward the *soil poultice* and a new separations methodology: Rebinding of macrocyclic metal complexes to molecularly imprinted polymers specifically templated via noncovalent interactions

X. ZUO, D. MOSHA, S.J. ARCHIBALD, A.K. MCCASLAND,
A.M. HASSAN, R.S. GIVENS and D.H. BUSCH*

Department of Chemistry, University of Kansas, Lawrence, KS 66045, USA

(Received 11 October 2004; in final form 25 October 2004)

The siderophore-based extraction of iron from the soil by bacteria is proposed as a model for a new separation methodology labeled the *soil poultice*, a molecular device that would selectively retrieve the complex of a targeted metal ion. In this first feasibility study we describe the synthesis and characterization of molecularly imprinted polymers based on noncovalent interactions, and their application in the specific recognition of macrocyclic metal complexes. The imprinting by salts of $\{N, N', N'', N'''\text{-tetra(2-cyanoethyl)cyclam}\}$ nickel(II) and $\{N, N', N'', N'''\text{-tetra(2-carbamoyl ethyl)cyclam}\}$ nickel(II) involves multiple hydrogen-bonding interactions when combined during copolymerization with the functional monomer acrylamide or with the crosslinking monomer *N,N'*-ethylenebisacrylamide. Good rebinding capacity for the imprinting metal complex was observed in both acetonitrile and water. Parallel experiments using the vinylsulfonate salt of either nickel(II) complex adds electrostatic interactions, and use of good coordinating groups as functional monomers (e.g. vinyl pyridines) adds a minor ligand component. Imprinted polymers using pairs of interactions (hydrogen bonding plus electrostatic attractions or hydrogen bonding plus minor ligand binding) exhibit greatly increased rebinding abilities, revealing a most promising synergism between pairs of supramolecular modes of attraction. Furthermore, imprinting the polymers with the β isomer of $\{N, N', N'', N'''\text{-tetra(2-carbamoyl ethyl)cyclam}\}$ nickel(II) perchlorate led to a marked preference for reuptake of the β isomer, exemplifying a substantial stereoselectivity. The reuptake of the β isomer was eight times that of the α isomer. The polymers are resistant to strong acids and oxidizing agents and show an increase in rebinding capacity during cycles of reuse. The affinities of the same ligands were determined for a number of metal ions, revealing high degrees of selectivity for Hg(II) and Cu(II). The imprinting procedure, combined with the accompanying selective chelation by macrocyclic ligands, supports the possibility of a new methodology for efficient extraction of metal ions under conditions not necessarily amenable to conventional techniques.

Keywords: Soil poultice; Molecularly imprinted polymers; Noncovalent interactions; Macrocyclic metal complexes

*Corresponding author. E-mail: busch@mail.ukans.edu

1. Introduction

Microbes satisfy their need for iron by secreting extremely powerful ligands called siderophores into their surroundings to extract iron from the iron oxides in the soil, after which the microbe's cell membrane selectively brings the iron-siderophore complex into its interior [1]. We see this natural system as a model for a new way of recovering metal ions from various sources, such as soil deposits and surface contaminations. Such a synthetic system requires a strongly binding, highly selective ligand and that requirement is clearly within the capabilities of modern coordination chemistry [2]. However, the system also requires the equivalent of the cell membrane that selectively adsorbs the targeted metal complex. Here we propose that a molecularly imprinted polymer can serve this purpose. For convenience in discussion we will call this synthetic system a "soil poultice," implying that this substance can be contacted with contaminated soil and, like a medicinal poultice, it will cure the ill represented by metal ion contamination.

Because of the great importance of molecular recognition and selective binding to both fundamental science and its many applications, molecularly imprinted polymers (MIPs, first introduced by Wulff and Sarhan in 1972 [3]) have received much attention in the fields of chemistry and analytical sciences [4]. In a molecular templating process, an imprint (or template) molecule is reversibly bound to functional monomers and copolymerized in a suitable solvent (porogen) with an excess of crosslinking monomer. Removal of the imprint affords tailored binding cavities that, ideally, are complementary in size, shape and functional group orientation to the imprint molecule. Thus, the resulting polymer can selectively rebind the original imprint in competition with its structural analogs or environmental competitors.

In our soil poultice, it is important that the guest, the metal complex, binds easily and smoothly with the imprinted polymer host. Based on the interactions between an imprint and functional monomers, MIPs can be divided into two groups: covalent and noncovalent. The rebinding capacity of covalent systems is high because of the strong covalent interaction, and often over 80% of the theoretical sites can be reoccupied. In comparison, the rebinding capacity of noncovalent systems (e.g. the combination of single-point hydrogen bonding and electrostatic interactions) has not previously exceeded about 20% [4f,5]. However, for many purposes noncovalent MIPs have distinct advantages, including easy and rapid removal of imprint and rapid rebinding. These features make noncovalent MIPs especially attractive for our soil poultice, as for well-known separation methodologies such as chromatography and solvent extraction. Consequently, we are applying the principles [2] of modern coordination chemistry and supramolecular chemistry in studies dedicated to learning how to optimize noncovalent binding by MIPs. For the reasons stated above, our focus is on imprinting by, and rebinding of, complete metal complexes.

Much less attention has been directed at metal-imprinted polymers than at polymers imprinted with organic compounds. Over 30 years ago, Nishide and Tsuchida reported an early study of ionic imprinting in the synthesis of chelating polymers [6]. More recently, Kuchen and Schram [7] and Garcia *et al.* [8] developed highly efficient cation imprinted polymers for Cu/Zn and Gd/La separations. Chen *et al.* [9] proposed a sandwich structure for bis{*N*-(4-vinylbenzyl)-1,4,7-triazacyclononane}zinc(II) in a polymer matrix, and Sharma *et al.* [10] have incorporated cobalt(II) dioxygen carriers in imprinted polymers. Typically in most work involving MIPs and metal complexes,

the ligand of interest is covalently incorporated in the polymer and any rebinding involves the reaction of the free metal ion with the ligand that is part of the polymer. In our novel metal extraction concept, MIPs rebind the *entire metal complex*, selectively, enhancing any selectivity the ligand may exhibit in binding to the targeted metal ion. This procedure provides two consecutive recognition events, a combination that, in principle, favors effective selectivity even in the presence of competing metal ions.

In this exploratory study we focus on determining the efficacy attainable through the use of different modes of supramolecular interactions and the synergism that may exist between those different kinds of interactions. Attention is given to the binding capacity of the substrate-free imprinted polymers, the selectivity of that reuptake process, the robustness of the polymers to repeated use, and the relationship of the binding behavior to the morphology of the polymer samples. The results show that dramatically better results are attainable with noncovalent substrate binding than would be expected on the basis of the literature on the subject.

2. Experimental

2.1 Materials

All reagents were obtained commercially and used without further purification. Hydrochloric acid (37%, 99.999% pure) and nitric acid (70%, 99.999% pure) for polymer digestion were purchased from Aldrich. The stock solution of all M(II) nitrates, except mercury(II), were standardized against EDTA (AR, Aldrich) using a copper electrode and calomel reference electrode. The stock solution of Hg(II) nitrate (Reagent Plus, 99.99+%; Aldrich) was prepared by accurate weighing. Carbonate-free solutions of sodium hydroxide (0.202 M) were standardized potentiometrically against potassium hydrogen phthalate. 3-Vinyl pyridine was prepared according to a literature procedure [11].

2.2 Measurements

NMR spectra were recorded on a Bruker DRX-400 spectrophotometer. Fast atom bombardment (FAB) mass spectra were obtained using a VG ZAB MS mass spectrometer equipped with a xenon gun and 3-nitrobenzyl alcohol (3-NBA) as the matrix material. Nickel analyses were carried out on a JY138 ULTRACE ICP-AES instrument. Surface area and porosity data were collected on a Gemini II 2370 surface area analyzer by the BET gas desorption method.

Potentiometric titrations were performed under N₂ at 25.0°C on a Brinkmann Metrohm 736GB Titrino instrument equipped with an ORION Ross combination electrode (model 81-02). The electrode was standardized by three-buffer calibration using the Titrino's internal standardization method.

Equilibrium measurements were made on 50.0 mL of ligand solution (0.5×10^{-3} M), first in the absence of metal ions and then in the presence of each metal ion. The [L]:[M] ratios were 1:1, and the ionic strength was maintained constant at 0.1 M (NaNO₃). The pH data were collected after addition of 0.01 mL increments of standard NaOH solution (with equilibration time of 20–60 s for all the metal ions studied except

nickel(II), *vide infra*). The titration data (pH vs. mL base) were collected in the Titrino's built-in software. Direct pH meter readings were used for calculation of the protonation and stability constants. The constants determined are mixed constants (also known as Brønsted constants) that involve the hydrogen ion activity and the concentrations of the other species. The protonation and stability constants were calculated by fitting the potentiometric data with the SUPERQUAD program [12]. Species distribution diagrams were generated with the aid of the HySS2 program [13].

2.3 Synthesis of the ligands and their nickel(II) complexes

All the ligands and nickel(II) complexes were synthesized by the methods of Wainwright [14] and Freeman *et al.* [15].

2.3.1 *N,N',N'',N'''*-Tetra(2-cyanoethyl)-1,4,8,11-tetraazacyclotetradecane (1). The ligand **1** was prepared by refluxing 1,4,8,11-tetraazacyclotetradecane (cyclam) and acrylonitrile [14]. Yield: 76%. ^1H NMR (CDCl_3): δ 1.6 (quintet, 4H), 2.4 (t, 8H), 2.55 (complex mult., 16H), 2.7 (t, 8H). ^{13}C NMR: δ 119.3, 51.7, 51.3, 51.2, 24.7, 16.4. Anal. Calcd. for $\text{C}_{22}\text{H}_{36}\text{N}_8 \cdot 0.5\text{H}_2\text{O}$: C, 62.7; H, 8.85; N, 26.6. Found: C, 62.8; H, 8.84; N, 26.4.

2.3.2 *N,N',N'',N'''*-Tetra(2-carbamoylethyl)-1,4,8,11-tetraazacyclotetradecane (2). This compound was prepared by refluxing 1,4,8,11-tetraazacyclotetradecane and acrylamide in methanol [15] and recrystallizing from ethanol/water (5/1). Yield: 50%. ^1H NMR (D_2O): multiplet centered around δ 2.60 ppm. ^{13}C NMR: δ 178.3, 51.1, 49.9, 46.9, 32.9, 20.1. Anal. Calcd. for $\text{C}_{22}\text{H}_{44}\text{N}_8\text{O}_4$: C, 54.5; H, 9.15; N, 23.1. Found: C, 54.4; H, 9.16; N, 22.9.

2.3.3 α -[Ni(1)](ClO₄)₂·H₂O (α -3). The α isomer of the nickel(II) complex of ligand **1** was prepared as a green solid by the room temperature reaction of (%) and nickel(II) perchlorate in acetonitrile [15]. Yield: 88%. Mass spec. (FAB/+ve): m/z 569 = $[\text{NiL}(\text{ClO}_4)]^+$, 516 = $[\text{NiL}(\text{ClO}_4)\text{-CH}_2\text{CHCN}]^+$, 470 = $[\text{NiL}]^+$, 413 = $[\text{L+H}]^+$. Anal. Calcd. for $\text{C}_{22}\text{H}_{38}\text{N}_8\text{O}_9\text{Cl}_2\text{Ni}$: C, 38.4; H, 5.57; N, 16.3. Found: C, 38.7; H, 5.42; N, 16.4.

2.3.4 β -[Ni(1)](ClO₄)₂·H₂O (β -3). The β isomer of compound **3** was prepared as a dark green solid by refluxing α -[Ni(1)](ClO₄)₂·H₂O in acetonitrile [15]. Yield: 75%. Mass spec. (FAB/+ve): m/z 569 = $[\text{NiL}(\text{ClO}_4)]^+$, 516 = $[\text{NiL}(\text{ClO}_4)\text{-CH}_2\text{CHCN}]^+$, 470 = $[\text{NiL}]^+$, 413 = $[\text{L+H}]^+$. Anal. Calcd. for $\text{C}_{22}\text{H}_{38}\text{N}_8\text{O}_9\text{Cl}_2\text{Ni}$: C, 38.4; H, 5.57; N, 16.3. Found: C, 38.2; H, 5.36; N, 16.3.

2.3.5 α -[Ni(2)](ClO₄)₂ (α -4). This α isomer was prepared as a green solid by the room temperature reaction of **2** and nickel(II) perchlorate in water [15]. Yield: 65%. Mass spec. (FAB/+ve): m/z 641 = $[\text{NiL}(\text{ClO}_4)]^+$, 570 = $[\text{NiL}(\text{ClO}_4)\text{-CH}_2\text{CHCONH}_2]^+$, 542 = $[\text{NiL}]^+$, 485 = $[\text{LH}]^+$. Anal. Calcd. for $\text{C}_{22}\text{H}_{44}\text{N}_8\text{O}_{12}\text{Cl}_2\text{Ni}$: C, 35.6; H, 5.98; N, 15.1. Found: C, 35.9; H, 6.04; N, 14.7.

2.3.6 β -[Ni(2)](ClO₄)₂ (β -4). The β isomer of $[\text{Ni}(2)](\text{ClO}_4)_2$ was prepared as a light blue solid by refluxing **2** and nickel(II) perchlorate in water [15]. Yield: 75%.

Mass spec. (FAB/+ve): m/z 641 = $[\text{NiL}(\text{ClO}_4)]^+$, 570 = $[\text{NiL}(\text{ClO}_4)\text{-CH}_2\text{CHCONH}_2]^+$, 542 = $[\text{NiL}]^+$, 485 = $[\text{LH}]^+$. Anal. Calcd. for $\text{C}_{22}\text{H}_{44}\text{N}_8\text{O}_{12}\text{Cl}_2\text{Ni}$: C, 35.6; H, 5.98; N, 15.1. Found: C, 35.3; H, 5.99; N, 14.6.

2.3.7 β -[Ni(2)](CH₂=CHSO₃)₂ · 2H₂O (β -5). This vinylsulfonate salt was prepared as a pink solid by refluxing **2** and nickel(II) vinylsulfonate in water. Yield: 27%. Mass spec. (FAB/+ve): m/z 649 = $[\text{NiL}(\text{CH}_2\text{CHSO}_3)]^+$, 578 = $[\text{NiL}(\text{ClO}_4)\text{-CH}_2\text{CHCONH}_2]^+$, 542 = $[\text{NiL}]^+$, 485 = $[\text{L+H}]^+$. Anal. Calcd. for $\text{C}_{26}\text{H}_{54}\text{N}_8\text{O}_{12}\text{S}_2\text{Ni}$: C, 39.4, ; H, 6.85; N, 14.1. Found (2 determinations): C, 39.8, 39.3; H, 6.81, 7.18; N, 13.3, 14.3.

2.4 Polymer synthesis

All the polymers were prepared by thermally initiated free radical polymerizations. Typically, a solution of metal complex (imprint, 4 mol%), acrylamide (functional monomer, 16 mol%) and ethylene glycol dimethacrylate (EGDMA, crosslinker, 80 mol%) or *N,N'*-ethylenebisacrylamide (EBA, crosslinker with functional groups; no acrylamide was used in this case, *vide infra*), in a mixture of acetonitrile and methanol, was placed in a polymerization tube and purged with Ar for 5 min, followed by addition of the solid initiator, azobis(isobutyronitrile) (AIBN). The mixture was again purged with Ar for 5 min and the tube was sealed under Ar. The reaction was carried out at 50°C for 24 h. Then the polymers were dried *in vacuo*, ground and sieved to a 75–125 μm particle size.

2.5 Rebinding experiments

The imprint was removed by Soxhlet extraction with acetonitrile (24 h). In addition, the polymers incorporating the vinylsulfonate anion were washed repeatedly with a methanolic ammonium chloride solution to exchange any remaining cationic imprinted complex. All the samples were then vacuum dried, and preweighed portions were digested in concentrated nitric acid for 12 h. Baseline values for residual nickel(II) in the extracted polymers were obtained from ICP analyses on these samples. To measure the imprint rebinding, a preweighed amount of extracted polymer was shaken in a 0.18 M acetonitrile solution of β -4 for 24 h and collected by filtration. The samples were digested in concentrated nitric acid over 12 h and the nickel concentration measured by ICP to determine the amount of nickel(II) complex rebound within the polymer matrix. These values were corrected for residual nickel by subtracting the previous baseline values. Rebinding values were reproducible within 5% and the quantities are reported in tables 2–7.

3. Results and discussion

In its final, fully functional form, the soil poultice will exert selectivity at two levels: first, in the binding of the metal ion by the ligand and, second, in the binding of the metal complex by the molecularly imprinted polymer. In the best case, selective binding at each of the two stages would be very strong, and the rate at which the binding occurs would be rapid. The present studies have focused on a small number

Table 1. Overall equilibrium constants ($\log \beta_{\text{MHL}}$) for the ligand **2** and its metal complexes at 25.0°C and $I=0.1 \text{ M NaNO}_3$.^a

	H(I)	Hg(II)	Cu(II)	Ni(II)	Pb(II)	Cd(II)	Zn(II)
$\log \beta_{011}$	9.289(4)						
$\log \beta_{021}$	17.985(2)						
$\log \beta_{031}$	26.297(8)						
$\log \beta_{101}$		18.44(2)	18.48(2)	6.42(5)	6.13(5)	6.29(1)	6.48(1)
$\log \beta_{111}$		–	–	–	13.35(4)	14.43(1)	15.64(1)
$\log \beta_{201}$		24.22(4)	23.74(3)	10.60(8)	–	–	–

^aThe numbers in parentheses represent the standard deviation in the last significant figure.

Table 2. Synthesis, characterization and nickel rebinding capacities of polymers.^a

Polymer	Crosslinker	I/F/C ^b	BET ^c (BJH ^d)	Ni reuptake (mg/g polymer)
P1 (control)	EGDMA	0/4/20	365 (0.51)	2.3
P2	EGDMA	0/4/20	332 (0.44)	3.5
P3 (control)	EGDMA	0/12/20	197 (0.42)	2.6
P4	EGDMA	1/12/20	179 (0.37)	10
P5 (control)	EBA	0/0/18	200 (0.56)	22
P6	EBA	1/0/18	121 (0.28)	38
P7	EBA	2/0/18	69 (0.24)	29
P8^e	EBA	9/0/18	89 (0.25)	25

^aInitiated by AIBN at 50°C, acetonitrile/methanol = 1/1 for **P1–P4**, **P8**, 2/1 for **P5–P7**. ^bMolar ratio of imprint (β -4) to functional monomer (acrylamide) to crosslinker. ^cBET surface area (m^2/g). ^dBJH cumulative pore volume for pores between 1.7 and 300 nm in diameter (mL/g). ^eTreated with concentrated nitric acid to further remove the residual nickel(II) after Soxhlet extraction.

Table 3. Synthesis, characterization and nickel rebinding capacities of polymers.^a

Polymer	Imprint	I/F/C ^b	BET ^c (BJH ^d)	Ni reuptake in MeCN ^e	Ni reuptake in H ₂ O ^e
P1 (control)	None	0/4/20	365 (0.51)	2.3	2.6
P2	β -4	1/4/20	332 (0.44)	3.5	2.1
P9	β -5	1/4/20	143 (0.14)	7.2	5.4
P10	β -5	2/4/20	41 (0.02)	3.0	–
P11 (control)	None	0/4/20	397 (0.59)	1.9	–
P12	β -5	1/4/20	108 (0.25)	5.7	–
P13 (control)	None	0/4/120	389 (0.47)	0.25	2.0
P14	β -4	1/4/120	381 (0.61)	0.33	2.4
P15	β -5	1/4/120	370 (0.41)	4.5	4.0
P16 (control)	None	0/4/70	–	0.68	1.8
P17	β -5	1/4/70	–	4.8	4.3

^aInitiated by AIBN at 50°C except **P11** and **P12** (ABDV at 40°C), acetonitrile/methanol = 1/1. ^bMolar ratio of imprint to functional monomer (acrylamide) to crosslinker (EGDMA). ^cBET surface area (m^2/g). ^dBJH cumulative pore volume for pores between 1.7 and 300 nm in diameter (mL/g). ^eUnits: mg/g polymer.

of broad but essential issues. Because covalent interactions tend to involve slow kinetics, we restrict attention to those intermolecular interactions that are noncovalent. The immediate issue then becomes “can noncovalent interactions be strong enough to produce the proposed new methodology?” The literature indicates that imprinting using, for example, hydrogen bonding or electrostatic interaction, instead of covalent binding, supports only 10 to 15%, certainly less than 20%, rebinding capacity. An equally compelling issue relates to the compatibility of the combined goals of selective

Table 4. Synthesis, characterization and nickel rebinding capacity of polymers.^a

Polymer	Functional monomer	I/F/C ^b	BET ^c (BJH ^d)	Ni reuptake (mg/g polymer)
P18	4-vinyl pyridine	1/1/20	–	1.1
P19 (control)	4-vinyl pyridine	0/2/20	420 (0.86)	2.2
P20	4-vinyl pyridine	1/2/20	393 (0.94)	2.5
P21	4-vinyl pyridine	1/3/20	–	5.3
P22	4-vinyl pyridine	1/4/20	332 (0.57)	7.2
P23 (control)	4-vinyl pyridine	1/6/20	315 (0.52)	4.6
P24	4-vinyl pyridine	1/6/20	296 (0.58)	14
P25	3-vinyl pyridine	1/4/20	363 (0.61)	3.2
P26	2-vinyl pyridine	1/4/20	313 (0.59)	0.17

^aInitiated by AIBN at 50°C, acetonitrile/methanol = 1/1, ^bMolar ratio of imprint (β -4) to functional monomer (vinyl pyridine) to crosslinker (EGDMA). ^cBET surface area (m²/g). ^dBJH cumulative pore volume for pores between 1.7 and 300 nm in diameter (mL/g).

Table 5. Rebinding capacity and stereoselectivity of polymers.^a

Polymer	Imprint	Reuptake of α -4 (mg Ni/g polymer)	Reuptake of β -4 (mg Ni/g polymer)	Selectivity (β/α)
P1 (control)	None	0.45	2.3	5.1
P2	β -4	0.45	3.5	7.8
P3 (blank)	None	1.9	2.6	1.4
P4	β -4	2.2	10	4.5
P27	β -3	0.20	0.86	4.3

^aInitiated by AIBN at 50°C, acetonitrile/methanol = 1/1 except **P27** (neat acetonitrile); functional monomer (acrylamide)/crosslinker (EGDMA) = 4/20 for **P1**, **P2** and **P27**, 12/20 for **P3** and **P4**.

Table 6. Rebinding capacity and stereoselectivity of polymers.^a

Polymer	Imprint	Reuptake of α -3 (mg Ni/g polymer)	Reuptake of β -3 (mg Ni/g polymer)	Selectivity (β/α)
P1 (control)	None	0.64	0.50	0.78
P2	β -4	0.31	0.49	1.6
P27	β -3	0.32	0.49	1.5

^aInitiated by AIBN at 50°C, acetonitrile/methanol = 1/1 for **P1** and **P2**, neat acetonitrile for **P27**; functional monomer (acrylamide)/crosslinker (EGDMA) = 4/20.

Table 7. Reuse of polymers.

Polymer	Treatment	Ni reuptake (mg/g polymer)					BET ^b (BJH ^c)	BET ^b (BJH ^c)
		#1	#2	#3	#4	#5	before #1	after #4 (#5)
P1 (blank)	SE ^a	2.3	2.8	2.6	2.1	–	365 (0.51)	373 (0.63)
P1 (blank)	37% HCl	2.2	3.1	3.4	3.8	4.2	365 (0.51)	365 (0.48)
P2	37% HCl	2.9	4.5	4.4	4.3	5.1	332 (0.44)	331 (0.68)
P2	70% HNO ₃	3.5	3.8	4.2	4.4	5.1	332 (0.44)	258 (0.36)
P22	70% HNO ₃	7.2	8.2	9.8	11	–	332 (0.57)	163 (0.36)

^aSoxhlet extraction. ^bBET surface area (m²/g). ^cBJH cumulative pore volume for pores between 1.7 and 300 nm in diameter (mL/g).

binding during complex formation and selectivity during the binding of the complex to the polymer. Furthermore, are these porous, imprinted polymers likely to be durable enough to be used in a separations methodology? In considering these issues the binding capacity has been studied at both the complex formation level and the polymer/imprint level for the first system of this kind.

3.1 Selectivity of macrocyclic metal complex formation

The complexing ability and metal ion selectivity of macrocyclic ligand **2** (chart 1) were investigated by equilibrium methods. Protonation constants for **2** and formation constants of **2** with Cu(II), Hg(II), Cd(II), Pb(II), Zn(II) and Ni(II) were determined by glass-electrode titration measurements. Typical titration curves of **2** with NaOH (with and without metal ion present) are shown in figure 1. It can readily be seen that the ligand presents three protonation constants, two having high values and one a low value (table 1). The last constant was not determined because its high acidity prevented a sufficiently accurate determination by potentiometric measurements. The rate of equilibration was rapid for all the metal ion complexes studied in this work, except that of nickel(II), and straightforward glass-electrode measurements yielded the formation constants, which are also shown in table 1. While the

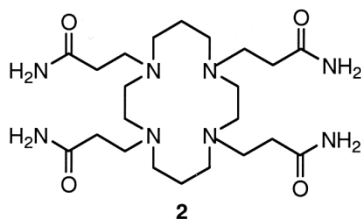


Chart 1.

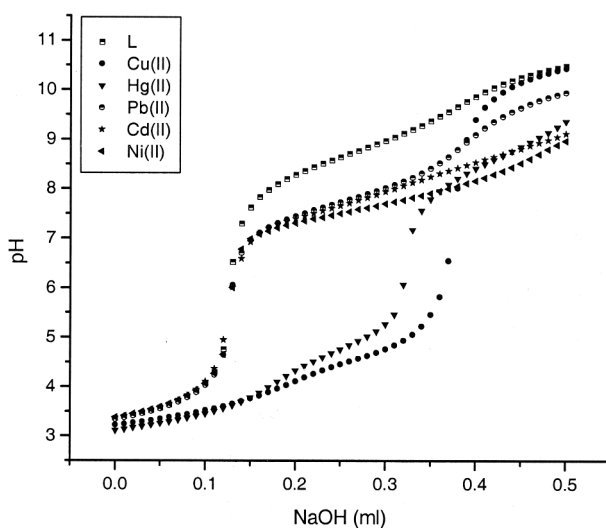


Figure 1. Potentiometric titration curves for **2** with and without M(II) at 25°C and $I=0.1$ M NaNO₃.

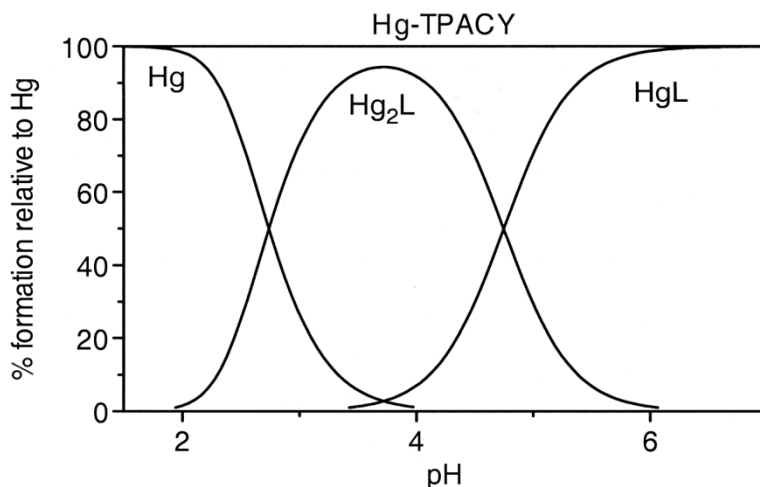


Figure 2. Species distribution diagram for solutions containing 1.0×10^{-3} M **2** and 1.0×10^{-3} M Hg(II) calculated with the HySS2 program.

nickel(II) complex was slow to equilibrate, it was not so slow as to render conventional glass-electrode measurements impractical. In all cases 1:1 complexes ML^{2+} were formed under the conditions of the measurements ($\log \beta_{101}$), whereas monoprotonated complexes MHL^{3+} were also found for Cd(II), Pb(II) and Zn(II). It is interesting that Cu(II) and Hg(II), which form complexes having the highest stability constants ($\log \beta_{101}$), also form dimers M_2L^{4+} . The species distribution diagram for Hg(II) is shown in figure 2. The large $\log \beta_{101}$ difference compared to other metal ions (>12) is indicative of very strong chelation to Cu(II) and Hg(II) [16]. This result for ligand **2** is especially promising for selectively binding these metal ions and possibly removing them from polluted sites. Equilibration of all metal ion complexes showed no precipitate even at high pH values, with the exception of Pb(II), which precipitated at $pH \sim 7$.

Because of their kinetic inertness, as was also shown in our previous study [17], the nickel(II) complexes with tetradentate tetraazamacrocyclic ligands are less likely to dissociate during the molecular imprinting process. Therefore, they have been used in all of the MIPs studies reported here.

3.2 Molecularly imprinted polymers

3.2.1 MIPs based on multiple and multisite hydrogen bonding: EGDMA vs. EBA. In the extensively investigated chiral separation of amino acid derivatives, a molar ratio of 1:4:20 (imprint to functional monomer to crosslinker) was found to be an optimized recipe for preparing noncovalent MIPs, using methacrylic acid as the functional monomer (approximately two- to threefold molar equivalents of the functional monomer relative to each polar group of the template) [18]. The maximum rebinding capacity was 10–15% [4f,5], as mentioned earlier.

In an effort to build strength into the noncovalent interactions, amide groups were chosen for our MIPs instead of carboxylic acid groups because they form stronger hydrogen bonds than carboxyl groups in polar solvents, such as acetonitrile [19]. Chart 2 (right) shows the interaction mode between the nickel(II) complex **4** (chart 3)

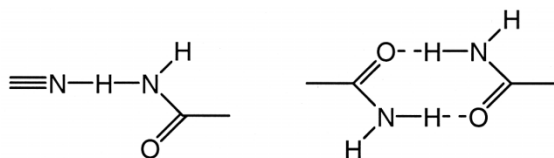


Chart 2.

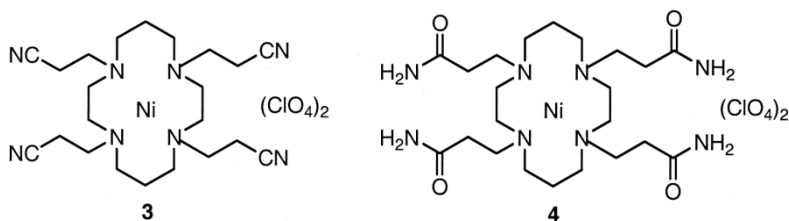


Chart 3.

and the functional monomer acrylamide. Pairs of amide groups form two-point hydrogen-bonding interactions, creating relatively strong four-center hydrogen-bonded linkages. In addition, the four pendant amide groups on the complex provide ample opportunity for hydrogen bonding with corresponding groups in the polymer. Both EGDMA and EBA were investigated as cross-linking agents. Whereas EGDMA can only serve as a proton acceptor in a hydrogen-bonding network, EBA adds both proton donors and proton acceptors to the hydrogen-bonding inventory.

First, we studied the MIPs imprinted against β -**4**, the thermodynamically stable isomer, because of its ready availability. Table 2 summarizes the synthetic parameters, surface characterization and rebinding capacity of the corresponding MIPs, as well as control polymers prepared with no imprint present. Generally, EGDMA polymers have significantly larger surface area and pore volume than EBA polymers. In both cases there was a decrease in surface area and pore volume with the incorporation of the imprint molecule.

The imprinted polymer **P2**, prepared with a molar ratio of 1 : 4 : 20 of β -**4** to acrylamide to EGDMA, showed a reuptake of 3.5 mg Ni/g polymer, or 26% rebinding of the theoretical sites. A noticeable imprinting effect was obtained when comparing this value to that (2.3 mg/g) of the control polymer **P1** (table 3). Because high functional monomer concentration favors the formation of an adduct between the imprint and the functional monomer [20], polymers with a 12 : 20 ratio of acrylamide to EGDMA were prepared (**P4**). Remarkably, the nickel(II) reuptake of the resulting imprinted polymer **P4** almost tripled the value previously determined for **P2**. The 12 : 20 control polymer **P3** also showed an increase in rebinding, but to a much smaller extent. Thus, the imprinting effect was more pronounced at a lower molar ratio of crosslinker to functional monomer. From these data we have learned that it is possible to produce high binding and rebinding capacities in MIPs by providing an abundance of amide-based, hydrogen-bonding sites. Capacities have been found that far exceed any reported previously.

Polymer recognition of the metal complex can also be realized with different specific positions and orientations of the hydrogen-bonding groups in the polymer; for example, the functional groups can be located on either the functional monomer or the crosslinker. EBA was introduced for two reasons. First, it was known that, under

most conditions, not all of the acrylamide enters into the polymerization and the presence of EBA could replace that loss of functional groups (acrylamide). Second, replacing EGDMA with EBA made it possible to learn the effect of increasing the number of amide groups in the polymers (two amide groups in each EBA molecule). Consequently, EBA polymers were prepared in the absence of the usual acrylamide “functional monomer.” The expected hydrogen bonding interaction pattern is the same as that of the EGDMA/acrylamide polymers (chart 2, right).

As shown in table 2, EBA polymers exhibited considerably higher nickel(II) reuptake than EGDMA polymers, reflecting the large excess of amide groups on the crosslinker. For such an imprinted polymer **P6** with 1 : 18 of β -4 to EBA, the nickel(II) reuptake was 38 mg/g, whereas the value for the control polymer was only 22 mg/g. This difference also demonstrates a marked increase in capacity based on the imprinting effect. However, further increases in the relative amount of imprint during the polymerization process resulted in lower rebinding capacity (**P7** and **P8**).

3.2.2 MIPs based on hydrogen bonding and electrostatic interaction: acetonitrile vs. water; Scatchard analysis. In studies on enantiomeric selectivity by MIPs it has been shown that the combination of electrostatic binding and hydrogen bonding can be made far more effective than either mode of interaction alone [4f]. We introduced the second mode of interaction, electrostatic attraction, by using the imprint β -5 with a polymerizable counter ion that can also be incorporated into the polymer. As shown in table 3, the rebinding capacity of the corresponding sample **P9** (1 : 4 : 20) amounted to 7.2 mg/g, or 54%, more than three times that of the control polymer **P1** and much higher than those reported in the literature for noncovalently imprinted polymers. The limited overall capacity of the polymer structure was again indicated; the otherwise similar polymer **P10**, with twice the amount of imprint, exhibited a lower nickel(II) reuptake. We note that this is associated with a substantial decrease in surface area and pore volume, suggesting that the impaired binding ability may arise from the altered morphology of the polymer.

As relatively weak noncovalent interactions are favored by lower temperature [21], 2,2'-azobis(2,4-dimethylvaleronitrile) (ABDV), a more reactive initiator than AIBN, was used to foster polymerization at 40°C, in place of the previous 50°C temperature. Unexpectedly, the imprinted polymer **P12**, as well as the control polymer **P11**, exhibited rebinding inferior to those of the AIBN-initiated polymers (table 3). Nevertheless, the nickel(II) reuptake by **P12** was still three times that of **P11**, again indicating the selective advantage of two synergistic interactions.

Even larger imprinting effects can be realized by preparing polymers at extremely high crosslinker to functional monomer ratios, e.g. 120 : 4 for EGDMA : acrylamide. The three polymers, **P13** (control), **P14** (hydrogen bonding alone) and **P15** (hydrogen bonding and electrostatic interaction) have surface areas and pore volumes so close in value that reasonable comparisons can be made with little doubt about the close similarities of their important morphologically dependent properties (e.g. availability of accessible sites). As shown in table 3, the samples whose binding is limited to hydrogen bonding alone, **P13** and **P14**, exhibited very poor rebinding capacity. This result is not surprising because the concentrations of amide groups in the polymers were greatly reduced. On the other hand, the nickel(II) reuptake by the polymer from two synergistic modes of interaction (hydrogen bonding and electrostatic attraction), **P15**, was enhanced by a factor of 18 compared to that of the control polymer. This is an excellent

example of imprint-enhanced rebinding capacity. In the absence of experiments directed at the competition between more than one candidate for complexation at the rebinding site, it is not clear that this improvement in binding should be described as an increase in the selectivity of the imprinted polymer.

All of the results described above come from studies using acetonitrile, both as the porogen (solvent present during polymerization) and as the medium for the rebinding experiments. Corresponding rebinding experiments have also been carried out in water, because water is the appropriate solvent for eventual deployment of the soil poultice. The rebinding behavior of these MIPs in water displayed three distinctive patterns: (1) The nickel(II) reuptake of control polymers exceeded that in acetonitrile, especially at high crosslinker ratios (**P13**, **P16**); (2) the nickel(II) reuptake in water of imprinted polymers that bind by hydrogen bonding alone is greater than that in acetonitrile at high crosslinker ratios (**P14**), but less than that in acetonitrile at low crosslinker ratios (**P2**); and (3) the nickel(II) reuptake by the imprinted polymers that benefit from both hydrogen bonding and electrostatic attractions is lower, relative to acetonitrile, at both high and low crosslinker ratios. It is interesting that in all cases in water, these (hydrogen bonding and electrostatic interaction) imprinted polymers bound about twice as much of the nickel(II) complex β -4 as did the control polymers. Good rebinding in water has also been reported in the molecular imprinting of biologically related compounds [22]. According to the literature [20,23], water is adverse with respect to hydrogen bonding and electrostatic interactions, while it is conducive to hydrophobic interactions, which play an important role in noncovalent binding.

Batch binding tests were also performed to examine the concentration dependence of rebinding to the imprinted polymers. The amount of β -4 bound to samples **P2** (hydrogen bonding alone) and **P9** (hydrogen bonding and electrostatic attractions) was plotted against free β -4 concentration to produce the binding isotherms (figure 3). It is clear from the binding data that **P9** possesses a substantially larger number of binding sites for β -4. Higher rebinding capacity at low concentrations implies that there are also

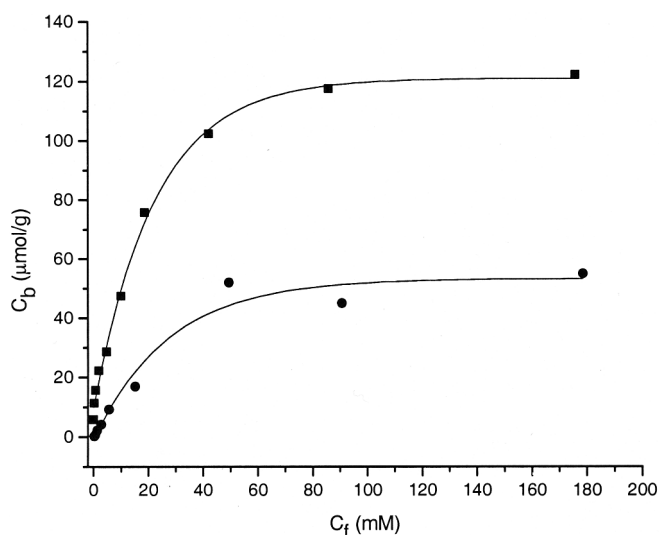


Figure 3. Binding isotherms of **P2** (●) and **P9** (■) in acetonitrile.

more strong binding sites in **P9**. The Scatchard plots, derived from the data shown in figure 3, reveal quite different binding properties for the two polymers. As shown in figure 4, the plot for **P9** is nonlinear with two straight lines fitting the Scatchard equation, indicating that there are two populations of binding sites with different affinities for the imprint molecule. The association constants, K_a , for the high- and low-affinity binding sites were calculated to be $(2.3 \pm 0.48) \times 10^3 \text{ M}^{-1}$ and $52 \pm 4.5 \text{ M}^{-1}$, respectively. By contrast, the Scatchard plot for **P2** (figure 5) appears to represent binding sites that are relatively homogeneous and of low-binding affinity

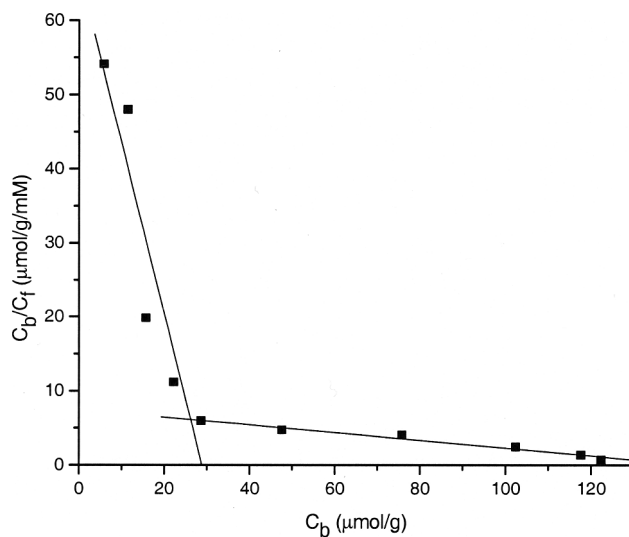


Figure 4. Scatchard plot of **P9** in acetonitrile.

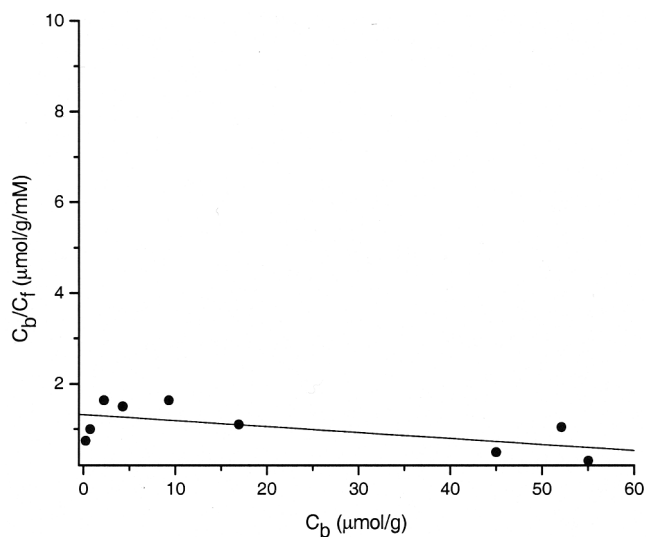


Figure 5. Scatchard plot of **P2** in acetonitrile.

($K_a = 13 \pm 6.1 \text{ M}^{-1}$). We rationalize these distinctly different binding sites in terms of the positioning of the copolymerized counter ions. The strong binding probably arises from sites enjoying both hydrogen-bonded linkages and the maximum presence of negatively charged sulfonate groups. The weak binding is attributed to sites having one or no counter ions in close proximity to the rebound cationic metal complex.

3.2.3 MIPs based on hydrogen bonding and minor ligand bonding. As functional monomers, vinyl pyridines provide supplementary ligating groups (the pyridine nitrogens) to bind to nickel(II), in addition to those on the primary ligand; e.g. **1** or **2**. Table 4 shows the nickel(II) reuptake of the polymers based solely on minor ligand interaction with various ratios of imprint, β -**4**, to vinyl pyridine. As was previously found for the hydrogen-bonding (only) polymers, a striking effect of excess functional monomer was observed. As the excess of 4-vinyl pyridine increased from 2:1 to 6:1, the rebinding capacity of the imprinted polymer increased from 2.5 to 14 mg/g and, at the same time, the imprinting effect became more pronounced.

The position of the vinyl substituent on the pyridine has a great influence on the rebinding capacity. Replacing 4-vinyl pyridine with 2-vinyl pyridine produced an “imprinted” polymer (**P26**) with essentially zero binding ability, and use of 3-vinyl pyridine yielded an intermediate value (compare **P25** with **P26** and **P22**). Thinking of the pyridine as a ligating function projecting out of the surface of a polymer mass, the accessibility of the corresponding nitrogen atom for binding to a metal atom would be expected to follow the order 4-vinyl pyridine > 3-vinyl pyridine > 2-vinyl pyridine, an expectation consistent with the observations.

When 4-vinyl pyridine was added as a second functional monomer (in addition to acrylamide), nickel(II) reuptake increased by a factor of two. Incrementally increasing the concentration of 4-vinyl pyridine by replacing an equivalent molar amount of acrylamide affords continuing improvement in the rebinding capacity (figure 6).

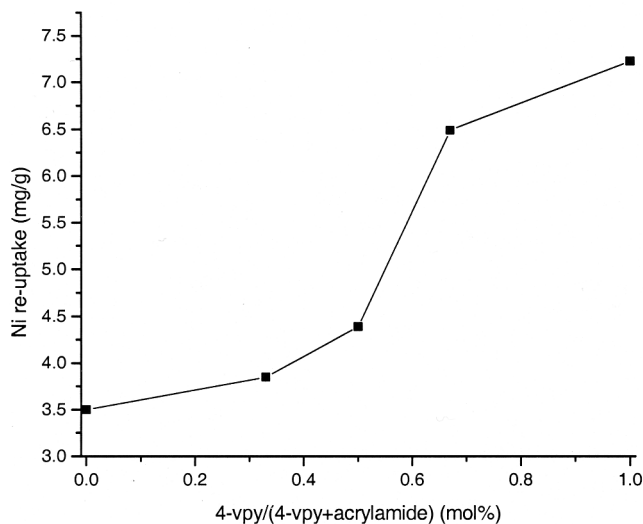


Figure 6. Rebinding capacity of the MIPs (AIBN, 50 °C; β -**4**/4-vinyl pyridine + acrylamide/EGDMA = 1/4/20).

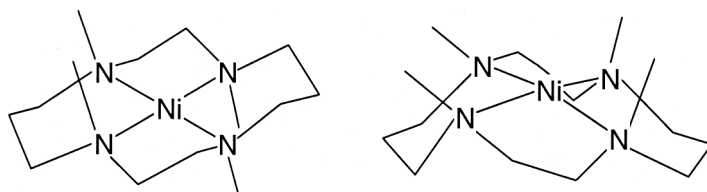


Chart 4.

Like the addition of a functional monomer capable of electrostatic attraction, this mode of interaction offers promise of synergistic bimodal binding of the macrocyclic metal complexes to the imprinted polymer.

3.2.4 Stereoselectivity of MIPs based on hydrogen bonding. The stereochemistry of macrocyclic metal complexes allows us to study the selective recognition of stereoisomers by molecular imprinting, which, to the best of our knowledge, has not previously been studied.

Earlier work revealed that the nickel complexes **3** and **4** (chart 3) exist in two isomeric structures (chart 4): The symbol β (**I**) is assigned to the thermodynamically favored form and α (**II**), to the kinetically favored form [15].

Based on the procedure of Barefield and coworkers [15], four nickel complexes, α -**3**, α -**4**, β -**3** and β -**4**, were prepared by the reaction of nickel perchlorate with the corresponding macrocyclic ligands at room and reflux temperatures. Considering the possibility of the transformation of the α isomer to the β isomer during the thermally initiated polymerizations, we focused on polymers imprinted by the β isomer in this work. The stereoselectivity is expressed as the ratio of β isomer to α isomer that was found to rebind to the β imprinted polymers.

As shown in table 5, all the imprinted polymers and control polymers had better rebinding capacities for β -**4**. It is noteworthy that β -**4** binds to the well-studied **P2** seven times more strongly than does α -**4**. The polymers (**P3** and **P4**) with lower cross-linker ratios (12:20) displayed increased rebinding of both α -**4** and β -**4**, albeit the stereoselectivity was decreased. Thus, the structure of imprints is crucial to the efficiency of imprinting and rebinding processes. Furthermore, the stereoselectivity of the control polymer **P1** (not imprinted) for β -**4** is 5.1. We must conclude that, beyond imprinting, the orientation of the pendant amide groups in β -**4** is more favorable for hydrogen bonding. It was not surprising to find that the β -**4** imprinted system was superior in binding affinity (0.86 mg/g for β -**4**) even with the sample **P27** imprinted with β -**3**, the complex having pendant nitrile groups on its ligand, rather than amide functions.

The rebinding by the two isomers of complex **3**, α -**3** and β -**3** (table 6), having pendant cyano groups rather than amide groups, was inferior. As a result, the aforementioned structure effect was not exhibited in the reuptake for complex **3**. The control polymer showed a higher affinity for α -**3** than did either imprinted polymer (**P2** or **P27**), and the rebinding of the isomers of complex **3** was indistinguishable for the polymers imprinted with either complex **3** or complex **4**. The inferior performance of complex **3** is not surprising because cyano groups form weaker hydrogen bonds (single-point, chart 2, left) than amide groups.

3.3. Reuse of polymers

Chemical stability is an important property of MIPs. Svenson and Nicholls recently studied the chemical stability of theophylline imprinted polymers that were based on the copolymerization of methacrylic acid and EGDMA [24]. The polymers retained their affinity ($\geq 95\%$) for the imprint on exposure (24 h) to 10 M hydrochloric acid. In this work, we studied the durability of the imprinted polymers by treating them with concentrated hydrochloric acid and, in separate experiments, with concentrated nitric acid, a very strong oxidizing agent.

For each cycle of reuse, a polymer sample was treated with the imprint β -4, then after digestion in acid it was washed repeatedly with water, methanol and dried *in vacuo* to remove the freshly bound β -4, in preparation for the next reuptake experiment.

As shown in table 7, the imprinted polymers **P2** and **P22** and the control polymer **P1** displayed increases in rebinding during reuse. The nickel(II) reuptake was enhanced by a factor of 1.5–2 in the fourth or fifth rebinding runs when the polymers had been treated with concentrated hydrochloric acid or nitric acid for about 50 h. Clearly, these polymers are quite resistant to strong and oxidizing acids.

The function of acid was indirectly evidenced by a reuse process based on Soxhlet extraction. In this process, the imprint was removed after each rebinding run. As shown in table 7, the nickel reuptake of **P1** was less in the first run and the value for the fourth run was even lower than that for the first run.

The mechanism by which acid treatment increases rebinding capacity remains unknown. Solid-state ^{13}C NMR analyses showed nearly identical spectra (figure 7) for the samples before and after nitric acid digestion [25], although the ester groups in EGDMA units are subject to hydrolysis under such harsh conditions [4f]. Elemental analyses showed an increase in nitrogen content after nitric acid treatment [26]. Furthermore, the color of the polymers changed from white to light yellow, supporting the possibility of the introduction of nitro groups, whose presence could bring about additional hydrogen bonding in the polymers.

Imprint removal with hydrochloric acid followed by Soxhlet extraction had no obvious influence on the polymer morphology. On the contrary, nitric acid treatment led to a marked decrease in surface area and pore volume (table 7).

4. Conclusions

These feasibility studies provide strong indications that the *soil poultice* concept may be realized sometime in the future. Success will depend on maximizing the rebinding capability and selectivity of MIPs designed specifically for the soil poultice. The requirements are very strong binding with great lability and our strategy to impart these properties on an MIP has been focused on optimizing combinations of the known supramolecular interactions; hydrogen bonding, electrostatic attraction and additional monodentate ligand binding. Using macrocyclic nickel complexes with pendant functional groups, we have developed MIPs having noncovalent rebinding capabilities that are much greater than previously observed. This clearly shows that the potential of labile, noncovalent binding MIPs has not yet been fully developed. In view of the limited attention that has been given to systems of this kind, these results are very promising.

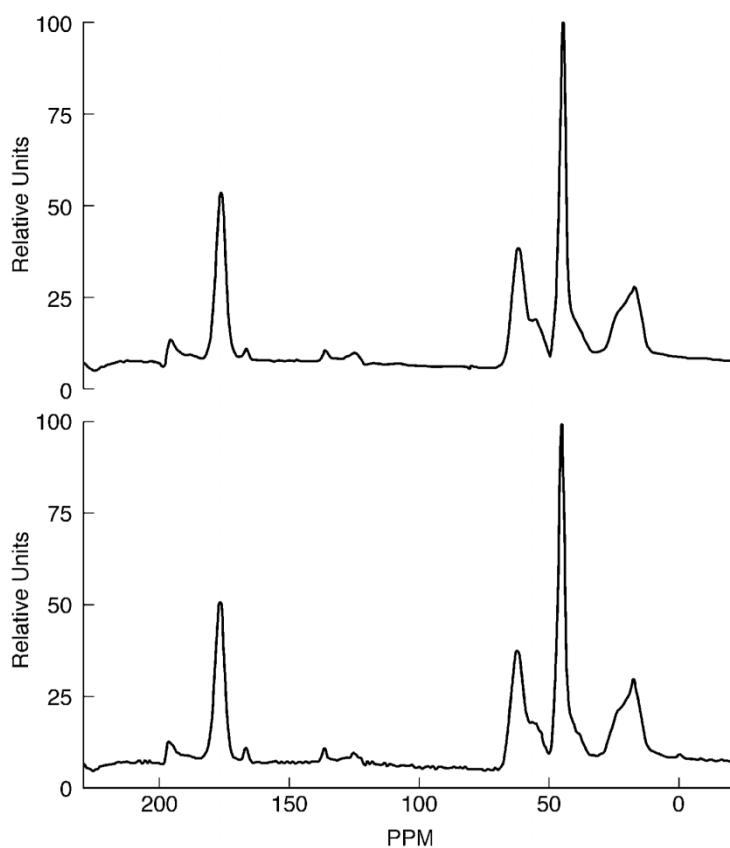


Figure 7. Solid-state ^{13}C NMR of **P1** before (bottom) and after (top) concentrated nitric acid treatment.

A general principle of the soil poultice is the dual selective processes that are built into the system: (1) chelate selectivity – that associated with metal ion binding to the ligands of choice; and (2) MIPs selectivity – that associated with selective adduct formation between the complex and the imprinted polymer. For the MIP studies themselves, low-spin, square-planar, substitution-inert nickel(II) complexes were used in these studies to avoid any complications, during polymerization, due to rapid dissociation of the imprinting complex.

The chelate selectivity of ligands used in the MIP studies was explored by determining the binding constants for a selection of metal ions. The protonation constants for the ligand **2** and the stability constants for the complexes of **2** with the labile metal ions Cu(II), Hg(II), Cd(II), Pb(II) and Zn(II) were determined. Complex **2** is highly selective toward Cu(II) and Hg(II) compared to the other metal ions, suggesting the possibility of using an MIP system based on **2** for recovering Cu(II) and/or Hg(II) from spills. These matters are the subject of ongoing investigations.

According to the literature, hydrogen-bonded MIPs have rebinding capacities limited to 10 to 15% of the available polymer sites. In our design, the first and simplest polymers depending on hydrogen bonding alone exceeded these limits substantially (~26%). We showed that, by careful choice and balance of the components

of the polymer, very large binding capacities can be achieved through hydrogen bonding alone – but that does not necessarily assure high selectivity.

Proceeding on the basis of leads provided by earlier studies on chiral substrates, we showed that synergism between pairs of supermolecular modes of binding can lead to very strong and selective substrate binding. With the combination of hydrogen bonding and electrostatic attraction, rebinding in excess of 50% is readily available. However, in many cases, the addition of imprints results in deleterious modifications in the polymer morphology. Under proper conditions the morphology can be maintained constant and the impact of binding group changes has been clearly demonstrated. Under such conditions, hydrogen bonding alone gives marginal results, as reported in the literature; however, the synergism between hydrogen bonding and electrostatic attraction produces ~ 20 times better rebinding. Careful control of composition and functional parameters can move these polymer materials from behavior properly described as not especially interesting to quite useful. The combination of a monodentate ligand delivered as a functional monomer in the polymer and a hydrogen-bonding functional monomer gives results parallel to those found for the hydrogen bonding plus electrostatic attraction duo.

All of the initial studies were carried out with acetonitrile as porogen. The ideal medium for a soil poultice is water. Remarkably, water is, at least in some cases, about 90% as good as acetonitrile when it comes to rebinding of substrates to the imprinted polymers, benefiting from two supramolecular modes of interaction. This is surprising in view of the expectation that water would be a poor solvent for hydrogen bonding and electrostatic interactions.

Some more detailed studies on systems having both electrostatic and hydrogen-bonding groups revealed two distinctive kinds of binding sites with affinities for substrates differing by a factor of 40–50 times. It is proposed that the strongly binding sites have a maximum positioning of vinyl sulfonate moieties in their near vicinities, as compared to the weaker sites. Furthermore, even the weaker site is some four times stronger than the binding sites in polymers linked to substrates by hydrogen bonding alone.

Stereoselectivity is evident and reflects the uniqueness of the macrocyclic complex imprinted systems. We have also shown that the rebinding capacity improves with reuse and that the MIPs are robust in the presence of oxidizing agents and strong acids.

Acknowledgments

The work was supported by the Department of Energy (Grant no. DE-FG07-96ER14708). We thank Dr Al-Ammr Assad Saleam for ICP analyses and Drs Christopher J. Lyon and Vidya Sagar Reddy-Sarsani for surface characterization. We are also grateful to Professor Eric J. Munson and Dr Joseph W. Lubach for their kind help in solid-state ^{13}C NMR analyses.

References and notes

- [1] (a) J.R. Telford, K.N. Raymond. In *Comprehensive Supramolecular Chemistry*, G. Gokel (Ed.), pp. 245–266, Pergamon, Oxford (1996); (b) J.R. Telford, K.N. Raymond. In *Bioinorganic Chemistry, An Inorganic Perspective of Life*, D. Kessissoglou (Ed.), pp. 25–37, Kluwer, Dordrecht (1995).

- [2] (a) D.H. Busch. In *The Complete Coordination Chemistry – What a Difference A Century Makes*, in Werner Centennial Volume, G.B. Kauffman (Ed.), ACS Symposium Series pp. 148–164, vol. 565, American Chemical Society, Washington, D.C. (1994); (b) D.H. Busch, In *Transition Metal Ions in Supramolecular Chemistry*, L. Fabbri and A. Poggi (Eds), pp. 55–79 Kluwer, Dordrecht (1994).
- [3] (a) G. Wulff, A. Sarhan. *Angew. Chem. Int. Ed. Engl.* **11**, 341 (1972); (b) G. Wulff, A. Sarhan, K. Zabrocki. *Tetrahedron Lett.* **14**, 4329 (1973).
- [4] For reviews see: (a) G. Wulff. *Chem. Rev.* **102**, 1 (2002); (b) K. Mosbach. *Anal. Chim. Acta.* **435**, 3 (2001); (c) B. Sellergren. *Angew. Chem. Int. Ed. Engl.* **39**, 1031 (2000); (d) M.J. Whitcombe, C. Alexander, E.N. Vulfson. *Synlett.* **6**, 911 (2000); (e) L.I. Andersson. *J. Chromatogr. B.* **745**, 3 (2000); (f) G. Wulff. *Angew. Chem. Int. Ed. Engl.* **34**, 1812 (1995).
- [5] (a) B. Sellergren. *Makromol. Chem.* **190**, 2703 (1989); (b) M. Kempe, K. Mosbach. *Anal. Lett.* **24**, 1137 (1991); (c) B. Sellergren, K.J. Shea. *J. Chromatogr.* **635**, 31 (1993).
- [6] N. Nishide, E. Tsuchida. *Makromol. Chem.* **177**, 2295 (1976).
- [7] W. Kuchen, J. Schram. *Angew. Chem. Int. Ed. Engl.* **27**, 1695 (1988)
- [8] R. Garcia, C. Pinel, C. Madic, M. Lemaire. *Tetrahedron Lett.* **39**, 8651 (1998).
- [9] H. Chen, M.M. Olmstead, R.L. Albright, J. Devenyi, R.H. Fish. *Angew. Chem. Int. Ed. Engl.* **36**, 642 (1997).
- [10] A.C. Sharma, V. Joshi, A.S. Borovik. *J. Polym. Sci. A: Polym. Chem.* **39**, 888 (2001).
- [11] S. Alumni, V. Laureti, L. Ottavi, R. Ruzziconi. *J. Org. Chem.* **68**, 718 (2003).
- [12] P. Gans, A. Sabatini, A. Vaca. *J. Chem. Soc. Dalton Trans.*, 1195 (1985).
- [13] L. Alderighi, P. Gans, A. Ienco, D. Peters, A. Sabatani, A. Vacca. *Coord. Chem. Rev.* **184**, 311 (1999).
- [14] K.P. Wainwright. *J. Chem. Soc., Dalton Trans.* 2117 (1980).
- [15] G.M. Freeman, E.K. Barefield, D.G. Van Derveer. *Inorg. Chem.* **23**, 3092 (1984).
- [16] The DOTAM (a cyclen-based ligand with four pendant groups $-\text{CH}_2\text{CONH}_2$) complexes of Cd^{2+} were described as six-coordinate with secondary coordination of the other two oxygen donors. H. Maumela, R.D. Hancock, L. Carlton, J.H. Reibenspies, K.P. Wainwright. *J. Am. Chem. Soc.* **117**, 6698 (1995).
- [17] (a) L.G. Warner, D.H. Busch. *J. Am. Chem. Soc.* **91**, 4092 (1969); (b) L.G. Warner, N.J. Rose, D.H. Busch. *J. Am. Chem. Soc.* **89**, 703 (1967).
- [18] D.J. O'Shannessy, L.I. Anderson, K. Mosbach. *J. Mol. Recog.* **2**, 1 (1989).
- [19] C. Yu, K. Mosbach. *J. Org. Chem.* **62**, 4057 (1997).
- [20] I.A. Nicholls, K. Adbo, H.S. Anderson, P.O. Anderson, J. Ankarloo, J. Hedin-Dahlström, P. Jokela, J.G. Karlsson, L. Olofsson, J. Rosengren, S. Shoravi, J. Svenson, S. Wikman. *Anal. Chim. Acta.* **435**, 9 (2001).
- [21] D.J. O'Shannessy, B. Ekberg, K. Mosbach. *Anal. Biochem.* **177**, 144 (1989).
- [22] L.I. Anderson, R. Müller, G. Vlatakis, K. Mosbach. *Proc. Natl Acad. Sci. USA*, **92**, 4788 (1995).
- [23] K. Adbo, H.S. Anderson, J. Ankarloo, J.G. Karlsson, M.C. Norell, L. Olofsson, J. Rosengren, J. Svenson, U. Örtengren, I.A. Nicholls. *Bioorg. Chem.* **27**, 363 (1999).
- [24] J. Svenson, I.A. Nicholls. *Anal. Chim. Acta.* **435**, 19 (2001).
- [25] The control polymer was selected to avoid the complication caused by the nitrogen-containing residue imprint (ca. 3% of the starting material) in the imprinted polymer.
- [26] The nitrogen content of **P1** is 1.59%. After the treatment with concentrated hydrochloric acid and concentrated nitric acid, the values are 1.40% and 2.08%, respectively.